

# Supplementary Information

## On-chip photonics and optoelectronics with van der Waals material dielectric platform

Xiaoqi Cui, <sup>\*a,b</sup> Mingde Du, <sup>a</sup> Susobhan Das, <sup>a</sup> Hoon Hahn Yoon, <sup>a,b</sup> Vincent Yves Pelgrin, <sup>a,c</sup> Diao Li <sup>a,b</sup> and

Zhipei Sun <sup>\*a,b</sup>

<sup>a</sup> Department of Electronics and Nanoengineering, Aalto University, Espoo FI-02150, Finland

<sup>b</sup> QTF Centre of Excellence, Department of Applied Physics, Aalto University, Espoo FI-00076, Finland

<sup>c</sup> Université Paris-Saclay, CNRS, Centre de Nanosciences et de Nanotechnologies,

91120, Palaiseau, France

Email: zhipei.sun@aalto.fi, xiaoqi.cui@aalto.fi

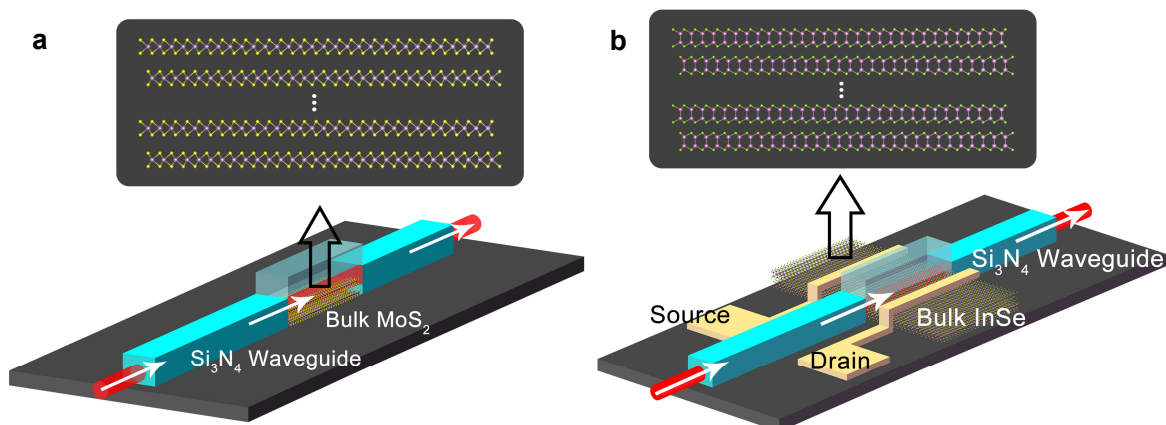


**Figure S1, The schemes of the MoS<sub>2</sub> integrated and InSe integrated devices. a** is the scheme of the MoS<sub>2</sub> integrated Si<sub>3</sub>N<sub>4</sub> waveguide, in which the Si<sub>3</sub>N<sub>4</sub> waveguide with a dimension of 6 μm width and 500 nm height is cladded by the SiO<sub>2</sub> at the bottom and the air at the sides and top. At the same time, the ~242 nm thick MoS<sub>2</sub> waveguide with an ultra-smooth surface is integrated into the Si<sub>3</sub>N<sub>4</sub> waveguide. Note that the width of the waveguide is designed as 6 μm because of the relatively low quality of the Si<sub>3</sub>N<sub>4</sub> films grown by the PECVD available in the group. **b** is the scheme of the InSe

integrated  $\text{Si}_3\text{N}_4$  waveguide, in which the width of the waveguide is also designed as  $6\ \mu\text{m}$  as in this case the waveguide allows multimode propagation with an acceptable linear loss ( $\sim 1.79\ \text{dB}\cdot\text{mm}^{-1}$  at  $532\ \text{nm}$ , as shown in Figure S7, the pure  $\text{Si}_3\text{N}_4$  waveguides are fabricated along with the InSe integrated ones following the same parameters).

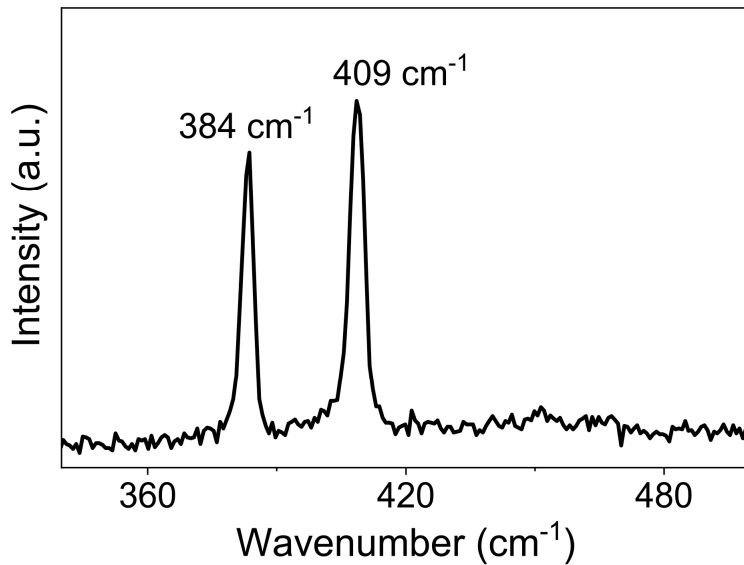


**Figure S2, Raman spectrum of the  $\text{MoS}_2$  waveguides.**

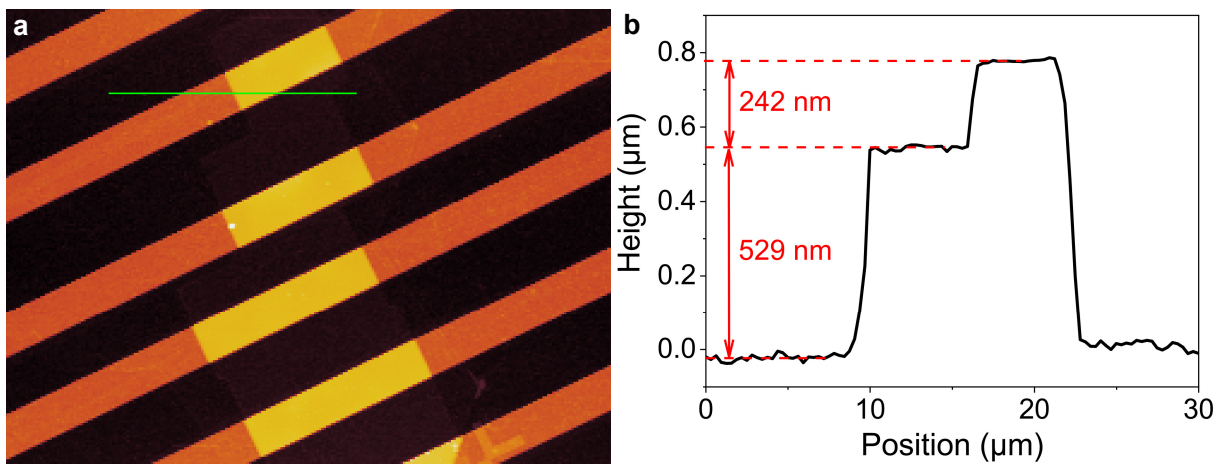


**Figure S3, AFM characterization of the  $\text{MoS}_2$  integrated devices. a** The AFM image and **b** the height profile corresponding to the section (indicated by the green line in **a**).

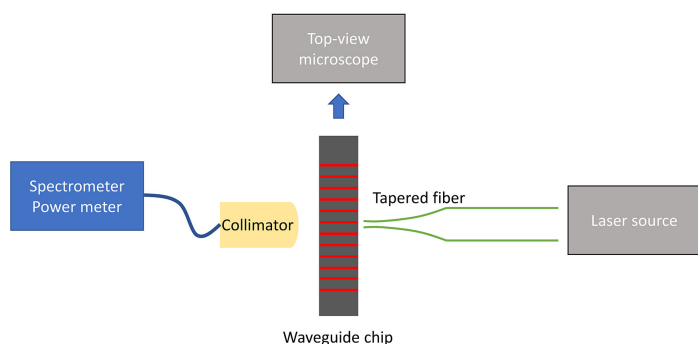


**Figure S4, Scheme of the homemade waveguide coupling system.**

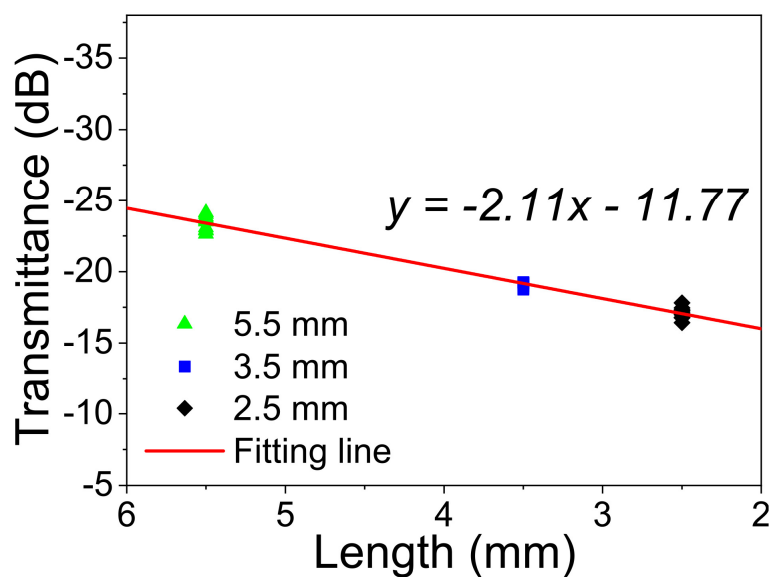


**Figure S5, Loss measurement results and linear fitting line of the pure  $\text{Si}_3\text{N}_4$  waveguides, which are fabricated together with the  $\text{MoS}_2$  integrated ones following the same parameters. The insertion loss and the linear loss of the  $\text{Si}_3\text{N}_4$  waveguide are 11.77 dB and 2.11 dB, respectively. The measurement is carried out by the cut-back method at 632 nm.**

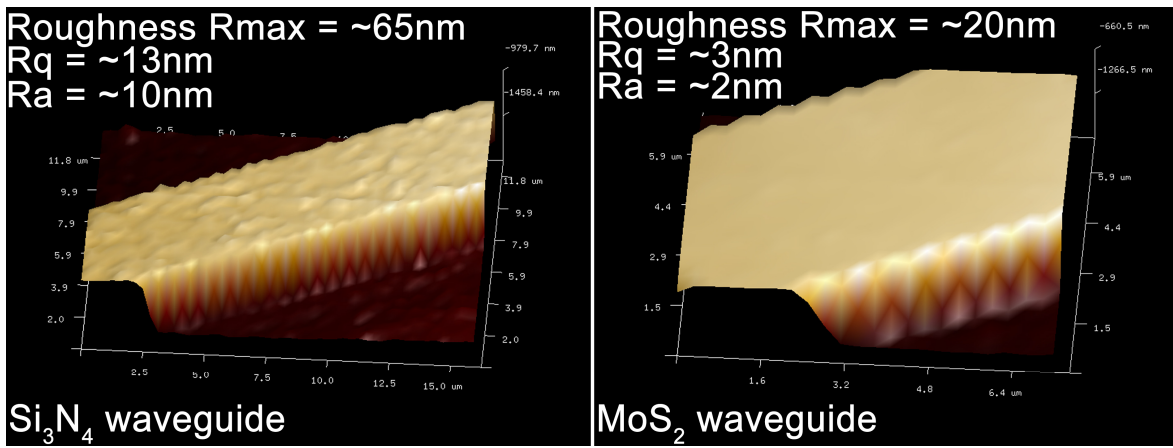


**Figure S6, Three-dimensional graphs of  $\text{Si}_3\text{N}_4$  waveguide and  $\text{MoS}_2$  waveguide measured by AFM.** The waveguides are fabricated together following the same parameters. The calculated roughness  $R_{max} = \sim 65\text{ nm}$ ,  $R_q = \sim 13\text{ nm}$ ,  $R_a = \sim 10\text{ nm}$  for  $\text{Si}_3\text{N}_4$  waveguides and  $R_{max} = \sim 20\text{ nm}$ ,  $R_q = \sim 3\text{ nm}$ ,  $R_a = \sim 2\text{ nm}$  for  $\text{MoS}_2$  waveguides, respectively.

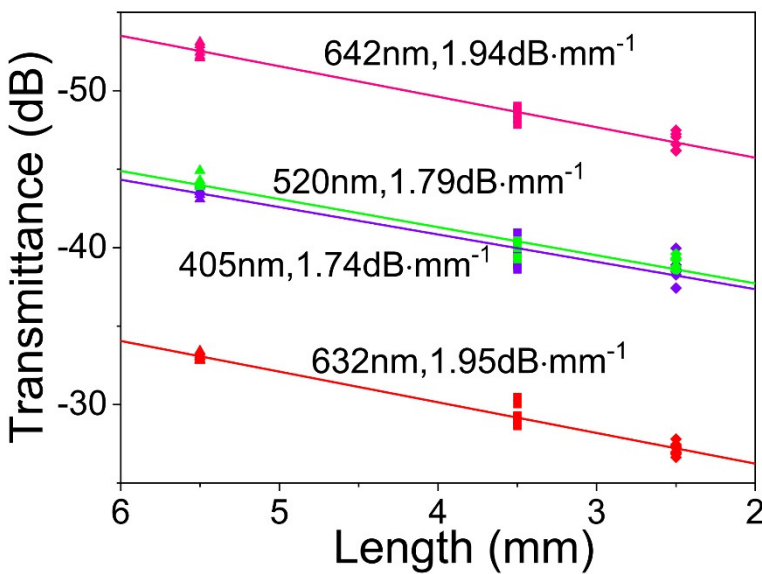


**Figure S7, Linear loss of  $\text{Si}_3\text{N}_4$  waveguides measured from the comparison sample which is fabricated along with the InSe integrated ones following the same parameters.** The measurement is carried out by cut-back method.

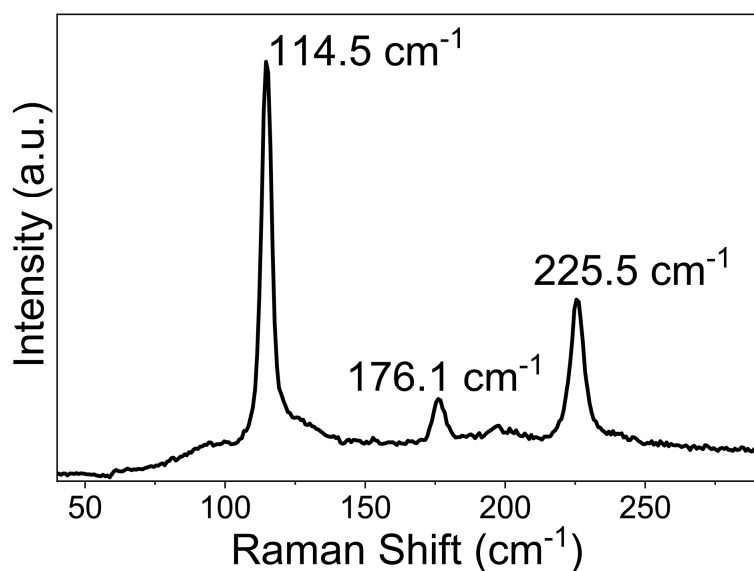


**Figure S8, Raman spectrum of the InSe flake.** The distinct InSe peaks at  $\sim 115 \text{ cm}^{-1}$ ,  $\sim 176 \text{ cm}^{-1}$ , and  $\sim 226 \text{ cm}^{-1}$ , corresponding to  $A_g$ ,  $E_g^2$ , and  $A_g^2$  phonon modes, respectively.

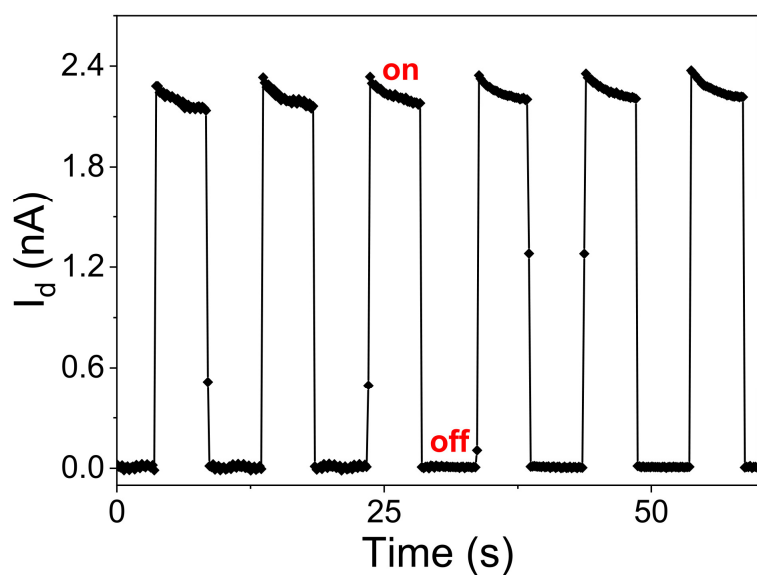


**Figure S9, Excitation-controlled measurement with 532 nm pump laser which is controlled in a 10-second on/off period.** The measurement is carried out using free-space coupling. From the diagram, one can clearly observe periodic on and off states of the drain current  $I_d$ , which corresponds to the laser on and off, respectively.

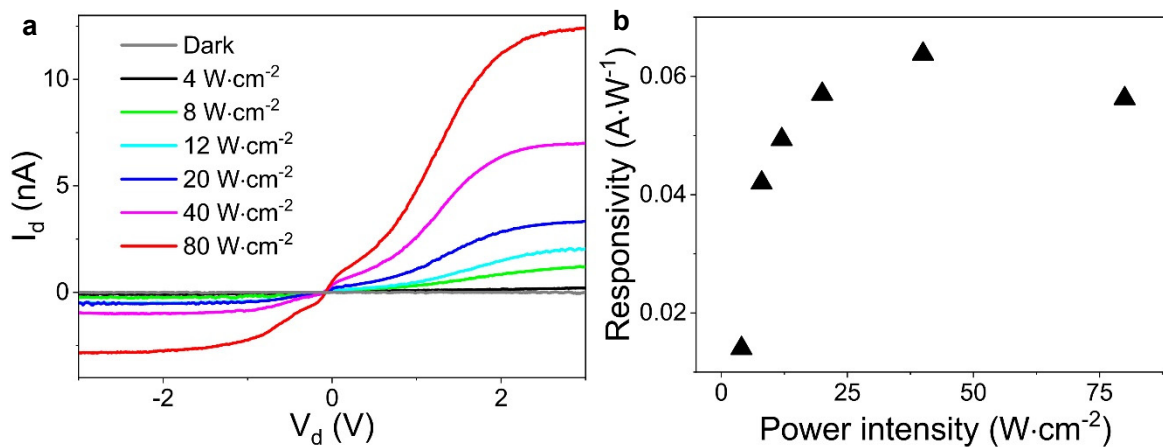


**Figure S10, Demonstration of on-chip photodetectors with vdW materials.** **a**  $I_d$ - $V_d$  curves of free-space coupling with 532 nm laser illumination,  $V_g=-60$  V; **b** the calculated photo-responsivity of free-space coupling at different incident intensity,  $V_g=-60$  V and  $V_d=2$  V. The free-space measurement is done in the WITec alpha300 system with a 20x objective (NA=0.4), the sample is connected to a print circuit board. Keithley 2401 and Keithley 2400 are used for applying source/drain and gate. The two source meter units are grounded and controlled by a homemade LabVIEW software for data collection.

According to the photocurrent mapping result (shown in the inset of Fig. 4a), the laser beam is focused on the highest photo-response area for the measurement. As shown in Fig. S10a,  $I_d$ - $V_d$  curves are collected at different incident intensity under the same gate voltage of -60V. When the laser illuminates on the flake, the drain current  $I_d$  shows clear dependence on the intensity, but the  $I_d$ - $V_d$  curves exhibit an apparent rectifying effect. This is due to the Schottky barrier at the surface of the flake and the Ti/Au electrodes. The photo-responsivity is calculated in the case of  $V_g=-60$  V and  $V_d=2$  V and plotted in Fig. S10b, in which the highest photo-responsivity is 0.06  $A \cdot W^{-1}$  at the intensity of  $\sim 40 W \cdot cm^{-2}$ .